

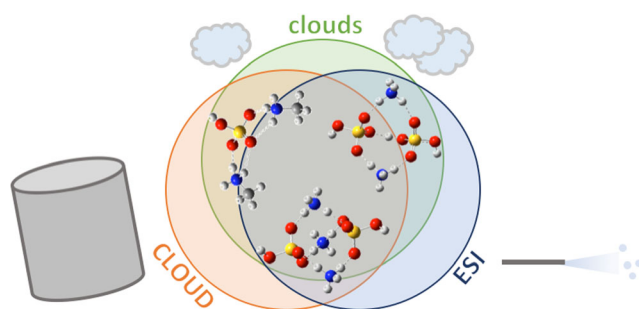


# Electrospray Ionization–Based Synthesis and Validation of Amine–Sulfuric Acid Clusters of Relevance to Atmospheric New Particle Formation

Sarah E. Waller, Yi Yang, Eleanor Castracane,  John J. Kreinbihl, Kathleen A. Nickson, Christopher J. Johnson 

Department of Chemistry, Stony Brook University, 100 Nicolls Road, Stony Brook, NY 11794, USA



**Abstract.** Atmospheric new particle formation (NPF) is the process by which atmospheric trace gases such as sulfuric acid, ammonia, and amines cluster and grow into climatically relevant particles. The mechanism by which these particles form and grow has remained unclear, in large part due to difficulties in obtaining molecular-level information about the clusters as they grow. Mass spectrometry–based methods using

electrospray ionization (ESI) as a cluster source have shed light on this process, but the produced cluster distributions have not been rigorously validated against experiments performed in atmospheric conditions. Ionic clusters are produced by ESI of solutions containing the amine and bisulfate or by spraying a sulfuric acid solution and introducing trace amounts of amine gas into the ESI environment. The amine content of clusters can be altered by increasing the amount of amine introduced into the ESI environment, and certain cluster compositions can only be made by the vapor exchange method. Both approaches are found to yield clusters with the same structures. Aminium bisulfate cluster distributions produced in a controlled and isolated ESI environment can be optimized to closely resemble those observed by chemical ionization in the CLOUD chamber at CERN. These studies indicate that clusters generated by ESI are also observed in traditional atmospheric measurements, which puts ESI mass spectrometry–based studies on firmer footing and broadens the scope of traditional mass spectrometry experiments that may be applied to NPF.

**Keywords:** New particle formation, Aerosols, Electrospray ionization, Ion source, Vibrational spectroscopy

Received: 7 June 2019/Revised: 12 August 2019/Accepted: 12 August 2019/Published Online: 10 September 2019

## Introduction

As a substantial source of atmospheric aerosol, new particle formation (NPF) plays an important role in health and climate [1, 2]. This process, by which atmospheric trace gases cluster and grow, has been observed in the ambient atmosphere [3–6], in atmospheric simulation chambers [7–10], and in flow

tube experiments [11–14]. These studies have identified sulfuric acid and nitrogen-containing bases as significant drivers of NPF, with particle formation rates depending most strongly on the concentration of sulfuric acid [9, 12–17]. Ammonia can stabilize the particles through salt bridge formation with sulfuric acid, and stronger bases such as dimethylamine are known to enhance growth rates, with particles containing both ammonia and dimethylamine growing the fastest [12, 18–21]. Recent studies have also suggested that diamines and organic acids may further stabilize new particles and enhance growth rates [14, 17, 22, 23].

Despite intensive study, important questions remain regarding the chemical mechanism by which new particles grow [24–

**Electronic supplementary material** The online version of this article (<https://doi.org/10.1007/s13361-019-02322-3>) contains supplementary material, which is available to authorized users.

Correspondence to: Christopher Johnson;  
e-mail: [chris.johnson@stonybrook.edu](mailto:chris.johnson@stonybrook.edu)

26]. The role of water is not well understood, even though it is ubiquitous in the atmosphere [22, 27, 28]. Structural questions such as the partitioning of ammonia and amines to the center or surface of the particles remain unclear [26]. The resolution of these molecular-level questions requires experimental probes sensitive to structure and intermolecular interactions that are not typically accessible with traditional atmospheric techniques such as particle sizing, counting, and online mass spectrometry.

The absence of molecular-level experimental insights has spurred the development of computational approaches to evaluate cluster structures and energetics, which serve as inputs to models predicting NPF rates [7, 29–35]. These models produce growth rates in the range of those observed in experiments, but their computational expense limits them to clusters of  $\sim 10$  molecules and concerns remain in confirming that the minimum energy structures are found [30, 31, 36, 37]. In order to produce molecular-level benchmarks for these calculations and to extend experiments beyond the size range currently tractable by theoretical methods, it will be necessary to develop experiments that provide enhanced control over cluster composition and measurements of their structures and thermodynamics.

To answer this need, experimental techniques developed for the study of ionic molecules and clusters have been applied to NPF. Mass spectrometry and ion mobility-based experiments have probed the ammonia-amine exchange mechanism [38, 39], the energetics of clusters with compositions relevant to NPF [29, 34–36, 40, 41], and their hydration [30–32, 42]. Spectroscopic investigations, particularly employing vibrational or photoelectron spectroscopy of mass-selected clusters, have elucidated structural information for clusters of sulfuric acid with water, amines, or organic acids [43–48]. However, the formation of clusters in these experiments, typically by electrospray ionization (ESI), is qualitatively different than in ambient atmosphere or in experiments simulating it, and thus, critical questions remain as to whether the clusters studied are truly representative of those found in the atmosphere.

Here we discuss methods for the synthesis of NPF-relevant ionic clusters in an ESI mass spectrometer. Our primary goal is to compare ESI-sourced clusters to those generated in chemical ionization mass spectrometers used in typical atmospheric measurements. We also introduce an approach to generate more complex multi-component clusters by exchange or addition of gaseous species introduced into the ESI environment and use vibrational spectroscopy to validate that these approaches yield the same cluster structures. These studies put ESI mass spectrometry-based studies on firmer footing and broaden the scope of traditional mass spectrometry experiments that may be applied to NPF.

## Methods

### *Sample Preparation*

For cation clusters, a 1 mM ammonium sulfate solution, aqueous in 50% methanol, was spiked with 0.01 vol% formic acid. To induce amine addition and substitution, two methods were

explored: aqueous introduction in the solution and gaseous introduction in the spray environment. For aqueous introduction, the three amines (methylamine, dimethylamine, and trimethylamine) were added separately to the ammonium sulfate solution, in a 1:2 ratio of ammonium sulfate:amine. For gaseous introduction, a reservoir containing aqueous amine was attached to the electrospray region of the instrument. A valve on the capsule isolating the amine capsule was opened slightly, allowing the amine to be slowly bled into the electrospray region.

For anion clusters, a 5-mM ammonium sulfate solution, aqueous in 50% methanol, was spiked with 0.1 vol% ammonium hydroxide. The abundance of these clusters was independent of concentration over the range of 1–10 mM, with higher concentrations yielding more unstable signal. A 25-mM aqueous sulfuric acid solution in 75% acetonitrile, similar to that suggested by Heine and coworkers, was used in experiments where the amine vapor was introduced [45].

### *Description of the Apparatus*

The instrument used for this work is a home-built guided ion beam/ion trap/tandem time-of-flight (TOF) photo-fragmentation mass spectrometer, which is shown diagrammatically in Figure 1. The ion source for the work described here is a micro-electrospray ionization interface housed inside a completely sealed, leak-tight chamber held near atmospheric pressure. This source is critical to the success of the experiments described here and will be discussed in more detail in the next section. Ionic clusters produced in the ESI source described below are introduced into the vacuum system through a 3.5-in.-long capillary with a 0.0625-in. outer diameter and a 0.0325-in. inner diameter and skimmed into an octopole ion guide that doubles as a room-temperature ion trap. From this trap, ions pass through a quadrupole mass filter featuring 0.75-in. rods and a 440-kHz power supply, providing mass selection up to 4000 amu/e. Next, ions pass through a LN<sub>2</sub>-cooled octopole ion trap capable of operation between room temperature and 80 K. For this study, the LN<sub>2</sub> octopole is operated at room temperature and as an ion guide. From here, they are turned 90° by an electrostatic quadrupole bender and guided to another octopole ion trap mounted to the 2nd stage of a cryogenic cold head with operation between 3 and 310 K. A mixture of gas (e.g., D<sub>2</sub>, H<sub>2</sub>O) is introduced into this trap via a Parker Series 9 pulsed valve attached to a 3/16-in. Teflon tube, thus stopping and collisionally cooling the ions.

After an appropriate amount of time, ions are extracted from the cryogenic trap through a tube lens and a 1D focusing and deflecting lens into an orthogonal-acceleration tandem TOF mass spectrometer. The accelerator, based on the arrangement of Wiley and McLaren [49], is pulsed to give a beam energy of  $\sim 4.1$  keV. Critically, the ions are accelerated towards ground, permitting all other times in the TOF to be referenced to ground. Ions at high energy are deflected and spatially focused by two sets of deflectors and einzel lenses and optionally mass-selected by a pulsed parallel-plate mass gate, reaching the time

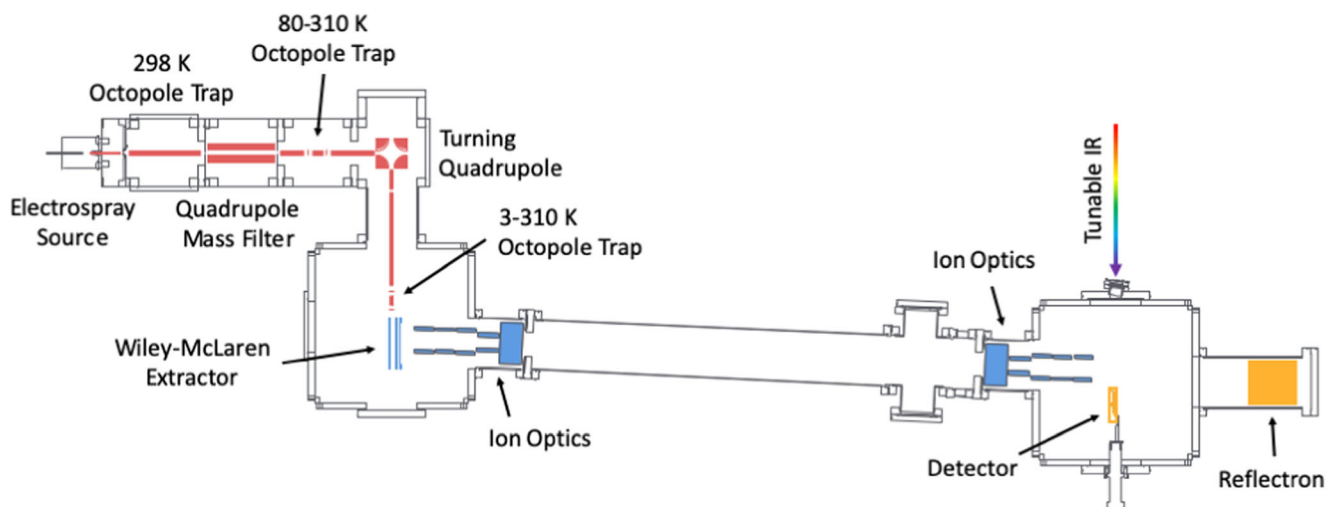


**Figure 1.** Schematic of the home-built photofragment mass spectrometer. The source components are highlighted red, the time-of-flight (TOF) components are blue, and the detector components are orange. Ions are created in a controlled electrospray environment and guided to a cryogenic ion trap that can be operated from 3 to 310 K. The ions are released from the trap and extracted into a tandem TOF mass spectrometer, where ions are guided and focused through a laser interaction region, and finally collide with a detector. The detector output is amplified, digitized, and saved by a computer. See text for more details

focus of the linear portion of the tandem TOF. At this point, the ions can be intersected by a pulsed, tunable IR laser directed parallel to the plane of the accelerator and retroreflected by a three-mirror arrangement for a total of four passes. Fragmented and unfragmented ions fly freely to a linear reflectron that separates and refocuses them in time on a 40-mm microchannel plate-based timing detector that is amplified by a factor of 100 by a 100-MHz AC-coupled amplifier. Typically, a mass resolution of 2000–3000  $M/\Delta M$  is obtained for this instrument, with the exact value depending strongly on the details of ion extraction from the cryogenic trap. Further resolution enhancement is expected by replacement of the single-stage reflectron with a two-stage device; however, the current resolution is sufficient for all experiments discussed here.

The electrospray source used in these experiments requires complete isolation of the spray atmosphere from the laboratory environment and is depicted in Figure 2. This is accomplished by construction of a vacuum-tight Teflon and polycarbonate cylindrical capsule with all joints sealed by Viton O-Rings. The capsule features a slip-seal flange permitting alignment of the emitter with the inlet capillary, typically in a collinear arrangement with a gap of approximately 2–10 mm. The emitter is a 360- $\mu\text{m}$  fused silica capillary pulled to 15 or 30  $\mu\text{m}$  inner diameter (New Objective Picotip). Stable ESI is typically achieved using voltages between 2 and 3 kV and solution flow rates of 0.2–0.6  $\mu\text{L}/\text{min}$ , yielding ESI currents of 100 nA–10  $\mu\text{A}$  and ion currents of several nA measured at the inlet. Dry and  $\text{CO}_2$ -purged compressed air or  $\text{N}_2$  is introduced into the chamber via a manual valve that can be metered to maintain a steady-state pressure near 1 atm. Additional reactant gases can be similarly introduced via similar ports arranged on the circumference of the capsule. This arrangement permits the use of toxic or noxious gases, such as the amines described here, without disruption of the laboratory atmosphere. Experience

has shown that the residence time of gas in the capsule is  $\sim 15$  s, and the time required to purge gases adsorbed on the inner surface of the capsule when switching reactant gases is approximately 1 h.

### Computational Methods

The structure and IR spectrum of the  $(\text{DMAH}^+)_3(\text{HSO}_4^-)_2$  cluster were calculated using the Gaussian 09 program suite for electronic structure calculations [50]. The combination of the CAM-B3LYP hybrid density functional and an aug-cc-pVTZ basis set was chosen due to its success in previous studies describing clusters with similar compositions and internal bonding [48]. An initial guess at the cluster structure was

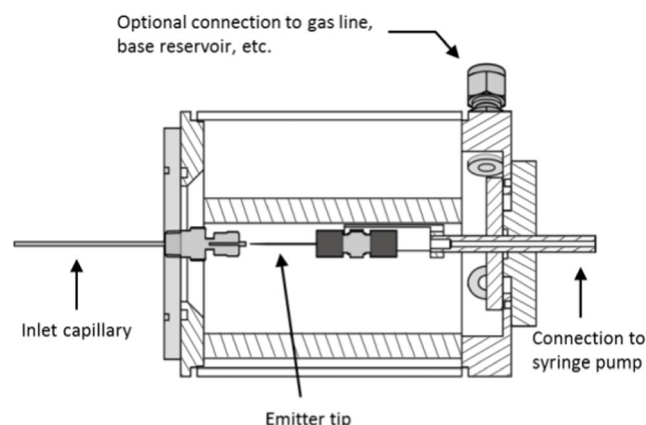


**Figure 2.** Side view of the electrospray source. Ions generated from the emitter tip pass into the first vacuum stage via an inlet capillary. The ESI environment is controlled by introducing various gases and/or vapors through compression fittings fitted with valves

based on the previously published (3,0,2) structure described by Johnson and coworkers [48, 51, 52]. The bridging ammonium molecules were replaced by dimethylammonium, with the methyl groups replacing non-hydrogen bonding hydrogens. The harmonic vibrational spectrum was obtained after a geometry optimization and is presented without the use of empirical scaling factors. The (0,3,2) and (3,0,2)<sub>DMA</sub> cluster structures can be found in the Supporting Information (S14).

## Results and Discussion

### Critical Features of the Electrospray Ionization Source

We first discuss the qualitative aspects of the ESI source used in these studies, as it enables source chemistry not amenable to those typically found on commercial instruments. This source is encapsulated in a sealed chamber, which can be held at variable pressures but is typically near 1 atm that is isolated from the ambient air. Dry air or N<sub>2</sub> is introduced via a manifold to replace air entering the vacuum system, but no other gas flows, such as nebulizing gas, are added. This allows reactant gases to also be introduced into the manifold with time to mix and reach steady state. The time required for this chamber to pump out via the vacuum system inlet is tens of seconds. Solutions are delivered to the ESI emitter via a fused silica capillary fed through a union embedded in the chamber wall, such that the solution is not exposed to the chamber atmosphere until it is sprayed.

### Cation Cluster Generation

For all cation clusters discussed here, the naming convention (*m,n*) denotes clusters of the form (NH<sub>3</sub>)<sub>*m*</sub>(H<sub>2</sub>SO<sub>4</sub>)<sub>*n*</sub>H<sup>+</sup>, while (*l,m,n*) indicates the number of constituents in a cluster (amine). *l*(NH<sub>3</sub>)<sub>*m*</sub>(H<sub>2</sub>SO<sub>4</sub>)<sub>*n*</sub>H<sup>+</sup> [51, 53]. Computational and experimental studies have shown that, in most cases, proton transfer is complete and the cluster constituents exist in maximally ionized forms such that the formulas of these clusters can be written as (aminium<sup>+</sup>)<sub>*l*</sub>(NH<sub>4</sub><sup>+</sup>)<sub>*m*</sub>(HSO<sub>4</sub><sup>-</sup>)<sub>*n*</sub> [26, 30, 54, 55]. These ionized clusters gain additional stability from Coulomb interactions between the ions, likely explaining the narrow distribution of ammonia molecules per sulfuric acid.

Typical distributions of clusters formed by ESI of ammonium sulfate solutions differ by charge. For cations, clusters with (NH<sub>4</sub><sup>+</sup>)<sub>*n*</sub>+<sub>1</sub>(HSO<sub>4</sub><sup>-</sup>)<sub>*n*</sub> are predominantly generated. Singly charged clusters with up to six bisulfate molecules and several doubly charged cation clusters are routinely produced in our source, as shown in Figure 3. Chemical ionization mass spectra from the CLOUD chamber primarily show clusters of the (*n*+1,*n*) and (*n,n*)H<sup>+</sup> formulas [18]. As seen in Figure 3, the (*n*+1,*n*) series are the dominant clusters generated by ESI. Lower intensity (*n,n*)H<sup>+</sup> clusters can also be observed. In our instrument, this second set of clusters are readily produced, presumably by collision-induced dissociation (CID) in the first room temperature octopole ion trap in our instrument, under harsh

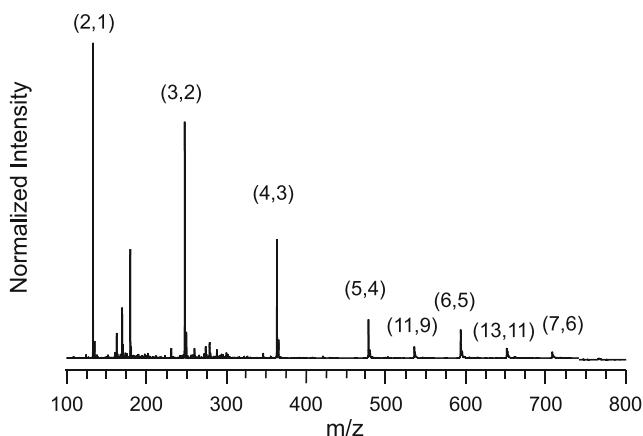


**Figure 3.** An overview of clusters generated by electrospray ionization of ammonium bisulfate solutions in positive mode. The (*m,n*) naming convention indicates the number of ammonia and sulfuric acid molecules comprising a cluster and is the form (NH<sub>3</sub>)<sub>*m*</sub>(H<sub>2</sub>SO<sub>4</sub>)<sub>*n*</sub>H<sup>+</sup>

source conditions. It was previously shown that loss of neutral ammonia is facile in these clusters under thermal decomposition, surface-induced dissociation, or infrared irradiation [48, 54, 56]. Recent studies of ionic liquid [57, 58], ammonium/dimethylammonium bisulfate [59], and bisulfate/sulfuric acid [60] cluster decomposition in atmospheric pressure interface mass spectrometers show that dissociation readily happens in the moderate-pressure region of the ion transport system. Thus, while the two ion sources produce essentially identical populations of ions, it is unclear whether each quantitatively reproduces those in the ambient CLOUD chamber. In fact, similar dissociation processes are likely occurring in the ion interfaces of both instruments. A similar set of clusters, albeit with a different set of relative intensities, was observed in a substantially different ESI source, suggesting that source-to-source variations may play a role in the relative abundances of the clusters but not in their identity [61]. Table 1 compares the cation cluster compositions formed via ESI and chemical ionization at the CLOUD chamber. The columns and rows indicate the number of ammonium and bisulfate molecules, respectively, in a cluster. For comparison with CLOUD, clusters generated from ESI have a green background while CLOUD clusters are outlined by bold, black borders. Clusters that are observed both from ESI and at CLOUD lie within the bold, black borders and are highlighted green. The vast majority of clusters formed from ESI are identical in composition to those detected at the CLOUD chamber.

### Amine Substitution in Cation Clusters

Amine incorporation or exchange has been proposed to substantially increase NPF rates compared with ammonia [13, 16, 35, 62]. In the studies presented here, two methods were used to create aminium-containing clusters. The simplest is ESI of a mixture of ammonium sulfate and an amine of interest (i.e., methylamine (MA); dimethylamine (DMA); or trimethylamine (TMA)). Alternatively, the same ammonium sulfate solution

**Table 1.**  $(\text{NH}_4^+)_m(\text{HSO}_4^-)_n$  Cation Clusters Generated from ESI (green) and from CLOUD (Outlined in Black). Columns Indicate the Number of  $\text{NH}_4^+$  Molecules and Rows Indicate the Number of  $\text{HSO}_4^-$  Molecules in a Cluster

		# $\text{NH}_4^+$ $\rightarrow$										
		0	1	2	3	4	5	6	7	8	9	10
# $\text{HSO}_4^-$ $\rightarrow$	1	0,1	1,1	2,1	3,1	4,1	5,1	6,1	7,1	8,1	9,1	10,1
	2	0,2	1,2	2,2	3,2	4,2	5,2	6,2	7,2	8,2	9,2	10,2
	3	0,3	1,3	2,3	3,3	4,3	5,3	6,3	7,3	8,3	9,3	10,3
	4	0,4	1,4	2,4	3,4	4,4	5,4	6,4	7,4	8,4	9,4	10,4
	5	0,5	1,5	2,5	3,5	4,5	5,5	6,5	7,5	8,5	9,5	10,5
	6	0,6	1,6	2,6	3,6	4,6	5,6	6,6	7,6	8,6	9,6	10,6
	7	0,7	1,7	2,7	3,7	4,7	5,7	6,7	7,7	8,7	9,7	10,7
	8	0,8	1,8	2,8	3,8	4,8	5,8	6,8	7,8	8,8	9,8	10,8
	9	0,9	1,9	2,9	3,9	4,9	5,9	6,9	7,9	8,9	9,9	10,9
	10	0,10	1,10	2,10	3,10	4,10	5,10	6,10	7,10	8,10	9,10	10,10

discussed above can be electrosprayed in the presence of amine vapor, yielding a distribution of partially or fully amine-substituted clusters. Mass spectra of clusters generated from amine solutions and by introducing MA, DMA, or TMA vapors into the electrospray environment are compared in Figures 4 and 5.

Figure 4 compares the distributions of clusters containing one bisulfate ion. Mass spectra are color-coded with  $\text{NH}_3$  in black, MA in red, DMA in blue, and TMA in purple. Clusters generated from amines in solution are presented upright, while mass spectra collected with amine vapors are inverted below their solution counterparts. Clusters with the same mass are formed when the amine is dissolved in solution and as when it is introduced in the ESI environment as a vapor. The inverted mass spectra presented in Figure 4 were collected by carefully controlling the amount of amine vapor introduced into the electrospray environment in order to create distributions with similar relative intensities to those produced via ESI. The exception to this is the TMA-containing clusters, which readily exchanges with ammonia at partial pressures below our ability to stably control in the current experimental setup.

The mass spectra of clusters containing two bisulfate molecules are presented in Figure 5. For MA and DMA substitution, clusters with identical masses are generated by both solution- and vapor-phase syntheses. However, no substituted TMA clusters are observed when TMA is introduced in the ESI solution, even for up to 16 equivalents of TMA. However, clusters with TMA are readily formed when TMA vapor is present. Additionally, a peak corresponding to the  $(3,0,1)_{\text{TMA}}$  cluster is observed, while no similar clusters are seen for MA or DMA. Cation clusters containing three bisulfate molecules formed by amine introduction in the ESI solution and as a vapor can be found in the Supporting Information (S13).

The lack of TMA-containing clusters in the solution-phase case is curious and allows us to speculate on the formation mechanism of these clusters from solution. We hypothesize that the key factor is the inability of TMA to form multidentate

hydrogen bonds, leading to substantial partitioning of it at the droplet surface. In the ion evaporation model of ESI, it could be expected that TMA-containing clusters would be readily made, as ions would last reside in the TMA-enriched interface. In the charge residue model of ESI, TMA would more likely evaporate and the resulting cluster would be expected to be TMA-poor. The observation of TMA-poor clusters points to the charge residue model, though it by no means proves it. In the likely case these clusters result from dissociation of larger clusters nascent from the spray, an alternative hypothesis can be proposed that suggests that cluster dissociation does not yield TMA-rich clusters of this size. This question remains unresolved in our setup.

The formation mechanism of the vapor-synthesized clusters is unclear. The fact that TMA-containing clusters could only be made using the vapor method suggests that vapors are not quickly diffusing into the volume of the droplet to yield nascent clusters that are already substituted. However, this does not rule out the possibility that surface-bound amines exchange with ammonia during ejection of ions from the droplet (in the ion ejection picture) or at the end of solvent evaporation (in the charge residue picture). The other likely scenario is that fully desolvated ammonium bisulfate clusters exchange with amines in the gas phase, much the same as they do in the ambient atmosphere. Bzdek et al. showed that, at high vacuum, exchange of DMA for ammonia was facile, while the reverse process occurred only minimally, suggesting that the vapor-phase process is plausible [39]. This picture is further complicated by the fact that, as discussed above, the clusters likely dissociate during transport in the mass spectrometer, and thus, it is unclear if exchange occurs at atmospheric or reduced pressures.

### Anion Cluster Generation

Anion clusters present three possible formation routes: (1) solution substitution, (2) vapor substitution, or (3) direct vapor

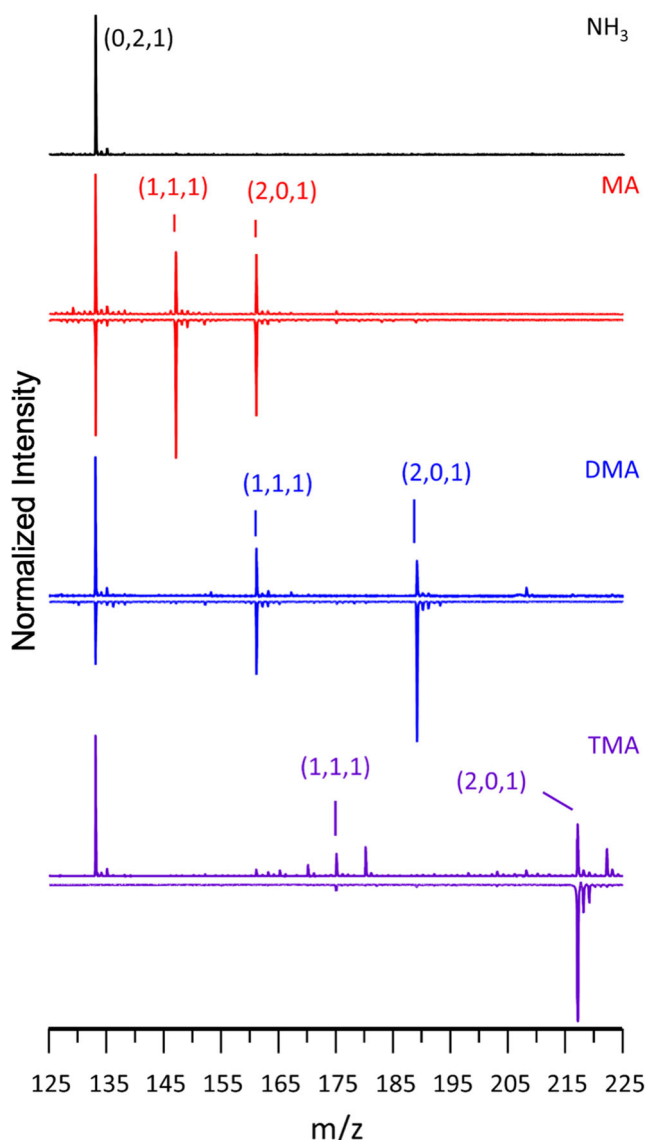


**Figure 4.** Aminium bisulfate clusters of the formula  $(\text{aminium}^+)_m(\text{NH}_4^+)_l(\text{HSO}_4^-)_1$  ( $m \leq 2$ ;  $l = 2 - m$ ) generated by ESI of an ammonium sulfate solution with added amine (upright) and by ESI of an ammonium sulfate solution sprayed in the chamber containing amine vapor (inverted). The ammonia ( $\text{NH}_3$ ) spectrum is presented in black; methylamine (MA) in red; dimethylamine (DMA) in blue; and trimethylamine (TMA) in purple

incorporation as described above for ammonia. Here we again use the notation  $(l,m,n)$  to denote cluster structure, except in the case of anions; the cluster is proton-deficient such that its formula is given by  $\{(\text{amine})_l(\text{NH}_3)_m(\text{H}_2\text{SO}_4)_n\} - \text{H}^+$ . The mass spectrum of an ammonium sulfate solution is presented at the top of Figure 6. At smaller sizes, clusters with very little ammonia are observed. For larger clusters, many as-yet unidentified low-intensity peaks appear. ESI of a sulfuric acid solution produces the second mass spectrum in Figure 6, which consists of clusters of the formula  $\text{HSO}_4^-(\text{H}_2\text{SO}_4)_n$ . We observe ion intensities for this approach that are typically 5–10

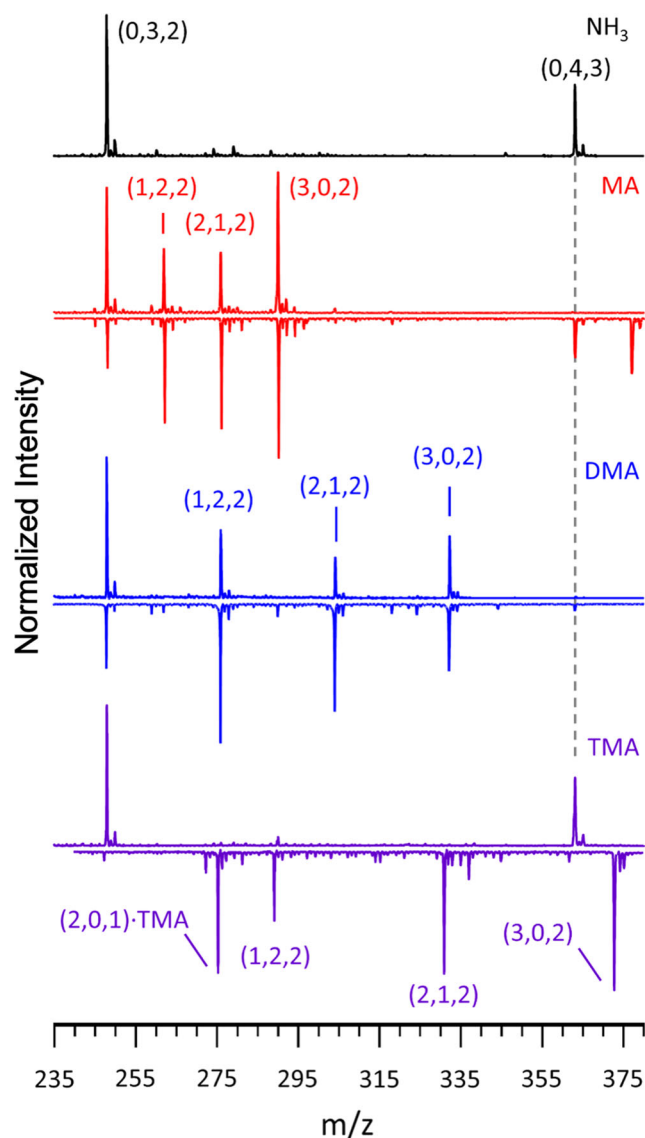


**Figure 5.**  $(\text{Aminium}^+)_l(\text{NH}_4^+)_m(\text{HSO}_4^-)_2$  ( $m \leq 3$ ;  $l = 3 - m$ ) clusters generated by ESI of an ammonium sulfate solution spiked with an amine (upright) and by ESI of an ammonium sulfate solution sprayed in an environment containing amine vapor (inverted). The ammonia ( $\text{NH}_3$ ) spectrum is presented in black; methylamine (MA) in red; dimethylamine (DMA) in blue; and trimethylamine (TMA) in purple. A small peak appears in the top TMA spectrum that appears coincident with the  $(1,2,2)$  TMA cluster below, but is actually a contaminant one mass unit higher

times larger than those for the ammonium sulfate solution. Addition of gaseous ammonia to the ESI environment yields the third mass spectrum in Figure 6, which shows the generation of ammonia-containing clusters for clusters  $(0,4)$  or larger. For each peak in this mass spectrum, a corresponding peak can be found in the ammonium bisulfate ESI spectrum, but the third mass spectrum is substantially less congested. Notably, the enhanced ion intensity gained through sulfuric acid ESI is

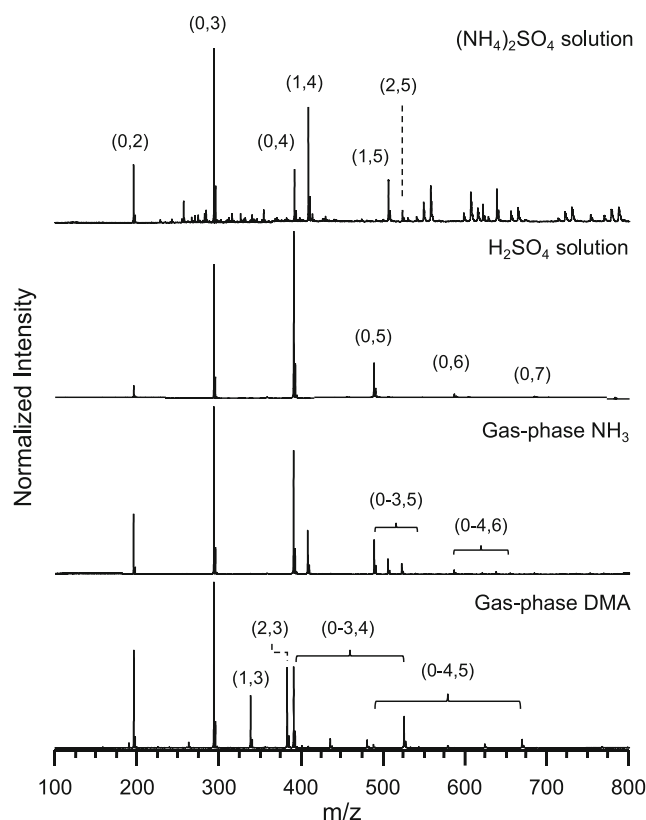


**Figure 6.** Comparison of anion mass spectra generated under different source chemistries. All labels follow the naming convention  $(n,m) = (\text{amine})_n(\text{sulfuric acid})_m$ . At the top is the mass spectrum of an ammonium sulfate solution, second is the mass spectrum of a sulfuric acid solution, and third and fourth are mass spectra taken with the same solution but with gaseous ammonia or dimethylamine introduced in the source, respectively. Detailed assignments of the smaller peaks in the top spectrum are given in the [Supplementary Information](#)

retained in this mass spectrum, such that this has become the preferred experimental approach in our laboratory.

Table 2 compares the anion cluster distributions observed from ESI-sourced clusters and the CLOUD chamber. Anion clusters generated by ESI exhibit a wider variety of compositions than cations, presumably due to the fact that they are richer in sulfuric acid and therefore contain more neutral constituents. The distribution observed by Bianchi and coworkers, outlined in black in Table 2, is in fact even broader. While it is not currently clear what the source of this discrepancy is, given that the ESI-generated clusters fall in the middle of the distribution of the CLOUD clusters, we postulate that these are likely the most stable clusters. Careful tandem mobility/mass spectrometry experiments have recently shown that the ion transport optics of a typical atmospheric pressure interface mass spectrometer used in laboratory and field measurements can lead to fragmentation of sampled ions [60]. It is possible that this fragmentation may account for some of the breadth of the distribution of clusters found in the CLOUD study for anions.

#### *Amine Substitution in Anion Clusters*

Anion clusters containing other amines can be produced in a similar fashion to the cation clusters. Clusters formed by exposing electro sprayed sulfuric acid to DMA vapor are indicated in Table 3. DMA-containing cluster distributions can be produced that closely resemble those measured at CERN (also indicated in Table 3). Furthermore, the addition of DMA vapor narrows the distribution of clusters for a given number of sulfuric acid molecules, producing clusters with lower sulfuric acid content (i.e., clusters with more ionic constituents), including some larger sized clusters with more amines than sulfuric acids. This likely results from enhanced stability of these clusters as compared with the ammonia-containing ones, as

**Table 2.**  $(\text{NH}_4^+)_m(\text{HSO}_4^-)_n$  Anion Clusters Generated from ESI of an Ammonium-Containing Solution (Green) and by Introducing Gaseous Ammonium into the ESI Environment (grey) and from CLOUD (Outlined in Black). Columns Indicate the Number of  $\text{NH}_4^+$  Molecules and Rows Indicate the Number of  $\text{HSO}_4^-$  Molecules in a Cluster

		# $\text{NH}_4^+$ →										
		0	1	2	3	4	5	6	7	8	9	10
← # $\text{HSO}_4^-$	1	0,1	1,1	2,1	3,1	4,1	5,1	6,1	7,1	8,1	9,1	10,1
	2	0,2	1,2	2,2	3,2	4,2	5,2	6,2	7,2	8,2	9,2	10,2
	3	0,3	1,3	2,3	3,3	4,3	5,3	6,3	7,3	8,3	9,3	10,3
	4	0,4	1,4	2,4	3,4	4,4	5,4	6,4	7,4	8,4	9,4	10,4
	5	0,5	1,5	2,5	3,5	4,5	5,5	6,5	7,5	8,5	9,5	10,5
	6	0,6	1,6	2,6	3,6	4,6	5,6	6,6	7,6	8,6	9,6	10,6
	7	0,7	1,7	2,7	3,7	4,7	5,7	6,7	7,7	8,7	9,7	10,7
	8	0,8	1,8	2,8	3,8	4,8	5,8	6,8	7,8	8,8	9,8	10,8
	9	0,9	1,9	2,9	3,9	4,9	5,9	6,9	7,9	8,9	9,9	10,9
	10	0,10	1,10	2,10	3,10	4,10	5,10	6,10	7,10	8,10	9,10	10,10

**Table 3.**  $(\text{DMAH}^+)_m(\text{HSO}_4^-)_n$  Anion Clusters Generated from ESI of Sulfuric Acid in the Presence of DMA Vapor (Blue) and from CLOUD (Outlined in Black). Columns Indicate the Number of  $\text{NH}_4^+$  Molecules and Rows Indicate the Number of  $\text{HSO}_4^-$  Molecules in a Cluster

		# DMAH <sup>+</sup> →										
		0	1	2	3	4	5	6	7	8	9	10
# HSO <sub>4</sub> <sup>-</sup> ←	1	0,1	1,1	2,1	3,1	4,1	5,1	6,1	7,1	8,1	9,1	10,1
	2	0,2	1,2	2,2	3,2	4,2	5,2	6,2	7,2	8,2	9,2	10,2
	3	0,3	1,3	2,3	3,3	4,3	5,3	6,3	7,3	8,3	9,3	10,3
	4	0,4	1,4	2,4	3,4	4,4	5,4	6,4	7,4	8,4	9,4	10,4
	5	0,5	1,5	2,5	3,5	4,5	5,5	6,5	7,5	8,5	9,5	10,5
	6	0,6	1,6	2,6	3,6	4,6	5,6	6,6	7,6	8,6	9,6	10,6
	7	0,7	1,7	2,7	3,7	4,7	5,7	6,7	7,7	8,7	9,7	10,7
	8	0,8	1,8	2,8	3,8	4,8	5,8	6,8	7,8	8,8	9,8	10,8
	9	0,9	1,9	2,9	3,9	4,9	5,9	6,9	7,9	8,9	9,9	10,9
	10	0,10	1,10	2,10	3,10	4,10	5,10	6,10	7,10	8,10	9,10	10,10

these clusters are expected to be composed of fewer neutral constituents. Anion clusters containing the same number of amines and sulfur-containing molecules necessarily feature doubly deprotonated  $\text{SO}_4^{2-}$  ions, if all amines are protonated, which may show substantially different reactivity and uptake properties from bisulfate as is typically found at these sizes.

### Structural Comparison

While we have shown that the clusters produced by gas- and solution-phase substitutions feature the same composition, it is not apparent that they have the same structure. Given that the formation mechanisms are likely to be quite different, we next look to determine their structures. Computational structure searches often find several low-energy structures with similar energies, and it is possible that during the rapid formation process of clusters in ESI, they may be kinetically trapped in higher lying isomers. Previous studies of the constituent identities and internal H-bonding networks indicate the presence of ammonium (and/or aminium) and bisulfate ions, which stabilize clusters through H-bonding and Coulomb interactions [48, 51, 52]. It is likely that exchange of ammonia in favor of an amine is generally energetically favorable, with the energetic gain increasing for more basic amines (all else being equal). This also raises the possibility that the cluster could become trapped in a local minimum geometry rather than relaxing into the global minimum, particularly if the mechanism for relaxation requires significant reorganization such as the breaking and reforming of multiple ionic hydrogen bonds.

In order to determine if the structures of clusters containing solution and vapor amines are the same, vibrational spectra of  $(\text{DMAH}^+)_3(\text{HSO}_4^-)_2 \cdot 2\text{D}_2$  clusters generated via both methods are compared in Figure 7. We chose the DMA-substituted cluster because DMA has the highest basicity of the amines that could be made via both mechanisms and thus might be the most likely to demonstrate a trapped local minimum geometry. The solution-amine spectrum is presented in black (middle),

and the vapor-amine spectrum in blue (bottom). Included at the top of Figure 7 is the calculated harmonic vibrational spectrum of the cluster as identified in previous spectroscopic studies [48, 54, 63].

The spectra of the clusters generated from solution- and vapor-phase amines are identical to within typical experimental variability. The peak positions between all vibrations are identical to within the laser bandwidth ( $\sim 5 \text{ cm}^{-1}$ ). However, the intensities of bands between 2500 and 3200  $\text{cm}^{-1}$  differ slightly, likely due to saturation effects as the laser power varies strongly as a function of frequency in this range. H-bonded stretches and modes corresponding to  $\text{CH}_3$ , indicated by an asterisk (\*), are labeled in gray. Distinct bisulfate stretching features are observed at the lowest energy ranges of the far-IR spectrum. The most pronounced features are assigned to the S–OH stretching (844  $\text{cm}^{-1}$ ), the symmetric  $\text{SO}_3$  stretching (1057  $\text{cm}^{-1}$ ), and the SOH bending (1119  $\text{cm}^{-1}$ ) vibrations. The  $\text{SO}_3$  asymmetric stretching vibrations cover a range of frequencies from 1165 to 1284  $\text{cm}^{-1}$ , with dimethylammonium bending modes observed at slightly higher frequencies. Two close-lying characteristic peaks associated with methyl groups are observed near 1485  $\text{cm}^{-1}$ . At higher energies, the bisulfate-free OH stretches are seen at 3798  $\text{cm}^{-1}$ , substantially red shifted from the harmonic prediction, as is typical for these modes. Hydrogen-bonded NH stretches span from 2792 to 3188  $\text{cm}^{-1}$ , and the feature seen centered at  $\sim 2520 \text{ cm}^{-1}$  arises from combination bands or overtones of lower energy vibrations. The notable intensity variation of this peak is also likely due to slight saturation in the top spectrum. The nearly identical match of the solution- and vapor-phase substituted cluster spectra suggests that the clusters have the same geometric structure. The structure of the (3,0,2)<sub>DMA</sub> cluster is similar to that of the (0,3,2) cluster determined previously and can be found in the Supporting Information (SI 4).

The IR spectra presented here indicate that the clusters produced from solution- and vapor-phase amines are identical in composition and structure, at least for the smaller clusters. It



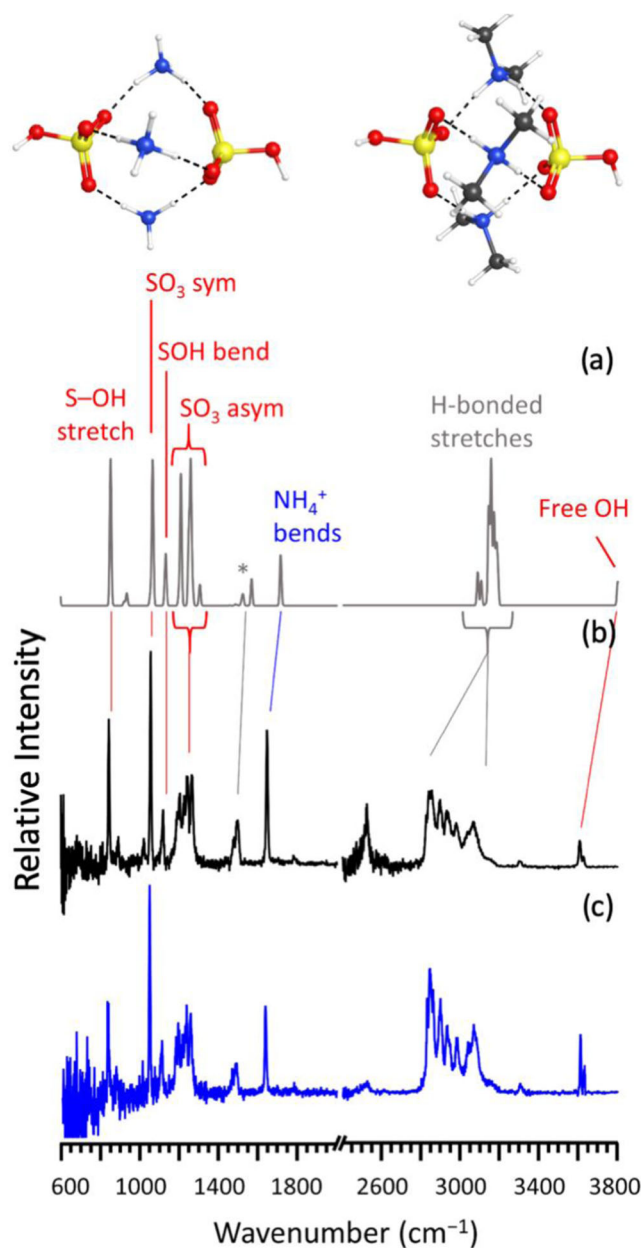


**Figure 7.**  $(\text{DMAH}^+)_3(\text{HSO}_4^-)_2 \cdot 2\text{D}_2$  cryogenic infrared vibrational predissociation spectra of clusters generated from a DMA-containing solution (middle) and by introducing DMA in the spray environment (bottom). Included at the top is the IR spectrum as predicted by DFT. For harmonic bands, the comparison between the experimental and theoretical spectra aid in identifying vibrational modes and the chemical moieties that give rise to them. Modes associated with bisulfate molecules are labeled in red, while dimethylammonium modes are labeled in blue. H-bonded stretches and  $\text{CH}_3$  modes have grey labels. Computed structures for  $(\text{NH}_4^+)_3(\text{HSO}_4^-)_2$  and  $(\text{DMAH}^+)_3(\text{HSO}_4^-)_2$  are shown at the top for reference

is worth noting that as clusters grow in size, it is likely that ammonium molecules will become fully hydrogen-bonded and reside in the cluster interior [36, 64]. In these cases, exchange of internal ammonia molecules with a vapor-phase amine will

be more difficult than directly forming clusters with amines in the ESI solution. Thus, solution- and vapor-phase structures may diverge at larger cluster sizes. This assumption is supported by our observation that solution-phase TMA does not readily form clusters with two sulfuric acids from ESI, while it does from vapor exchange. Which approach produces more atmospherically relevant clusters depends on the yet-unknown interplay between uptake and exchange in the NPF mechanism.

## Conclusions

We have discussed several approaches to generate ammonium bisulfate clusters of relevance to atmospheric new particle formation and have validated these approaches against clusters generated via chemical ionization in the atmospheric simulation chamber CLOUD. In all cases, we find that it is preferable to generate the simplest clusters via ESI and subsequently exchanging more complex amines by introducing their vapors into the ESI environment. Additionally, some clusters containing amines with lower hydrogen bonding numbers can only be made via vapor exchange. Infrared spectroscopy of clusters generated by either vapor exchange or ESI solution produce identical structures. These results place studies in which NPF-relevant clusters are generated via ESI on firmer ground and indicate that laboratory-based mass spectrometry techniques are effective means to gain insight into NPF-relevant processes.

## Acknowledgements

The authors received funding from the National Science Foundation under grant CHE-1566019 and Stony Brook University.

## Compliance with Ethical Standards

*Conflict of Interest* The authors declare that they have no competing interests.

## References

- Rückerl, R., Schneider, A., Breitner, S., Cyrys, J., Peters, A.: Health effects of particulate air pollution: a review of epidemiological evidence. *Inhal. Toxicol.* **23**, 555–592 (2011)
- Stocker, T., Qin, D., Plattner, G., Tignor, M., Allen, S., Boschung, J., Nauels, A., Xia, Y., Bex, V., Midgley, P. Cambridge Univ. Press, Cambridge and New York (2013)
- Nash, D.G., Baer, T., Johnston, M.V.: Aerosol mass spectrometry: an introductory review. *Int. J. Mass Spectrom.* **258**, 2–12 (2006)
- Zhao, J., Eisele, F.L., Titcombe, M., Kuang, C.G., McMurry, P.H.: Chemical ionization mass spectrometric measurements of atmospheric neutral clusters using the cluster-CIMS. *J. Geophys. Res. Atmos.* **115**, D08205 (2010)
- Jokinen, T., Sipilä, M., Junninen, H., Ehn, M., Lönn, G., Hakala, J., Petäjä, T., Mauldin III, R.L., Kulmala, M., Worsnop, D.R.: Atmospheric sulphuric acid and neutral cluster measurements using CI-API-TOF. *Atmos. Chem. Phys.* **12**, 4117–4125 (2012)
- Kulmala, M., Kontkanen, J., Junninen, H., Lehtipalo, K., Manninen, H.E., Nieminen, T., Petäjä, T., Sipilä, M., Schobesberger, S., Rantala, P., Franchin, A., Jokinen, T., Järvinen, E., Äijälä, M., Kangasluoma, J., Hakala, J., Aalto, P.P., Paasonen, P., Mikkilä, J., Vanhanen, J., Aalto, J.,

- Hakola, H., Makkonen, U., Ruuskanen, T., Mauldin, R.L., Duplissy, J., Vehkamäki, H., Bäck, J., Kortelainen, A., Riipinen, I., Kurtén, T., Johnston, M.V., Smith, J.N., Ehn, M., Mentel, T.F., Lehtinen, K.E.J., Laaksonen, A., Kerminen, V.-M., Worsnop, D.R.: Direct observations of atmospheric aerosol nucleation. *Science*. **339**, 943–946 (2013)
7. Dunne, E.M., Gordon, H., Kürten, A., Almeida, J., Duplissy, J., Williamson, C., Ortega, I.K., Pringle, K.J., Adamov, A., Baltensperger, U., Barmet, P., Benduhn, F., Bianchi, F., Breitenlechner, M., Clarke, A., Curtius, J., Dommen, J., Donahue, N.M., Ehrhart, S., Flagan, R.C., Franchin, A., Guida, R., Hakala, J., Hansel, A., Heinritzi, M., Jokinen, T., Kangasluoma, J., Kirkby, J., Kulmala, M., Kupce, A., Lawler, M.J., Lehtipalo, K., Makhmutov, V., Mann, G., Mathot, S., Merikanto, J., Miettinen, P., Nenes, A., Onnela, A., Rap, A., Reddington, C.L.S., Riccobono, F., Richards, N.A.D., Rissanen, M.P., Rondo, L., Samela, N., Schobesberger, S., Sengupta, K., Simon, M., Sipilä, M., Smith, J.N., Stozhkov, Y., Tomé, A., Tröstl, J., Wagner, P.E., Wimmer, D., Winkler, P.M., Worsnop, D.R., Carslaw, K.S.: Global atmospheric particle formation from CERN CLOUD measurements. *Science*. **354**, 1119–1124 (2016)
  8. Kim, J., Ahlm, L., Yli-Juuti, T., Lawler, M., Keskinen, H., Tröstl, J., Schobesberger, S., Duplissy, J., Amorim, A., Bianchi, F., Donahue, N.M., Flagan, R.C., Hakala, J., Heinritzi, M., Jokinen, T., Kürten, A., Laaksonen, A., Lehtipalo, K., Miettinen, P., Petaja, T., Rissanen, M.P., Rondo, L., Sengupta, K., Simon, M., Tomé, A., Williamson, C., Wimmer, D., Winkler, P.M., Ehrhart, S., Ye, P., Kirkby, J., Curtius, J., Baltensperger, U., Kulmala, M., Lehtinen, K.E.J., Smith, J.N., Riipinen, I., Virtanen, A.: Hygroscopicity of nanoparticles produced from homogeneous nucleation in the CLOUD experiments. *Atmos. Chem. Phys.* **16**, 293–304 (2016)
  9. Kürten, A., Li, C., Bianchi, F., Curtius, J., Dias, A., Donahue, N.M., Duplissy, J., Flagan, R.C., Hakala, J., Jokinen, T., Kirkby, J., Kulmala, M., Laaksonen, A., Lehtipalo, K., Makhmutov, V., Onnela, A., Rissanen, M.P., Simon, M., Sipilä, M., Stozhkov, Y., Tröstl, J., Ye, P., McMurry, P.H.: New particle formation in the sulfuric acid–dimethylamine–water system: reevaluation of CLOUD chamber measurements and comparison to an aerosol nucleation and growth model. *Atmos. Chem. Phys.* **18**, 845–863 (2018)
  10. Wagner, R., Yan, C., Lehtipalo, K., Duplissy, J., Nieminen, T., Kangasluoma, J., Ahonen, L.R., Dada, L., Kontkanen, J., Manninen, H.E., Dias, A., Amorim, A., Bauer, P.S., Bergen, A., Bernhammer, A.K., Bianchi, F., Brilke, S., Mazon, S.B., Chen, X., Draper, D.C., Fischer, L., Frege, C., Fuchs, C., Garmash, O., Gordon, H., Hakala, J., Heikkinen, L., Heinritzi, M., Hofbauer, V., Hoyle, C.R., Kirkby, J., Kürten, A., Kvashnin, A.N., Laurila, T., Lawler, M.J., Mai, H., Makhmutov, V., Mauldin III, R.L., Molteni, U., Nichman, L., Nie, W., Ojdanic, A., Onnela, A., Piel, F., Quéléver, L.L.J., Rissanen, M.P., Samela, N., Schallhart, S., Sengupta, K., Simon, M., Stolzenburg, D., Stozhkov, Y., Tröstl, J., Viisanen, Y., Vogel, A.L., Wagner, A.C., Xiao, M., Ye, P., Baltensperger, U., Curtius, J., Donahue, N.M., Flagan, R.C., Gallagher, M., Hansel, A., Smith, J.N., Tomé, A., Winkler, P.M., Worsnop, D., Ehn, M., Sipilä, M., Kerminen, V.M., Petäjä, T., Kulmala, M.: The role of ions in new particle formation in the CLOUD chamber. *Atmos. Chem. Phys.* **17**, 15181–15197 (2017)
  11. Zollner, J.H., Glasoe, W.A., Panta, B., Carlson, K.K., McMurry, P.H., Hanson, D.R.: Sulfuric acid nucleation: power dependencies, variation with relative humidity, and effect of bases. *Atmos. Chem. Phys. Discuss.* **12**, 1117–1150 (2012)
  12. Jen, C.N., McMurry, P.H.: Stabilization of sulfuric acid dimers by ammonia, methylamine, dimethylamine, and trimethylamine. *J. Geophys. Res. Atmos.* **119**, 7502–7514 (2014)
  13. Glasoe, W.A., Volz, K., Panta, B., Freshour, N., Bachman, R., Hanson, D.R., McMurry, P.H., Jen, C.N.: Sulfuric acid nucleation: an experimental study of the effect of seven bases. *J. Geophys. Res. Atmos.* **120**, 1933–1950 (2015)
  14. Jen, C.N., Bachman, R., Zhao, J., McMurry, P.H., Hanson, D.R.: Diamine-sulfuric acid reactions are a potent source of new particle formation. *Geophys. Res. Lett.* **43**, 867–873 (2016)
  15. Chen, M., Titcombe, M., Jiang, J., Jen, C., Kuang, C., Fischer, M.L., Eisele, F.L., Siepmann, J.I., Hanson, D.R., Zhao, J., McMurry, P.H.: Acid–base chemical reaction model for nucleation rates in the polluted atmospheric boundary layer. *Proc. Natl. Acad. Sci.* **109**, 18713 (2012)
  16. Almeida, J., Schobesberger, S., Kürten, A., Ortega, I.K., Kupiainen-Määttä, O., Praplan, A.P., Adamov, A., Amorim, A., Bianchi, F., Breitenlechner, M., David, A., Dommen, J., Donahue, N.M., Downard, A., Dunne, E., Duplissy, J., Ehrhart, S., Flagan, R.C., Franchin, A., Guida, R., Hakala, J., Hansel, A., Heinritzi, M., Henschel, H., Jokinen, T., Junninen, H., Kajos, M., Kangasluoma, J., Keskinen, H., Kupce, A., Kurtén, T., Kvashnin, A.N., Laaksonen, A., Lehtipalo, K., Leiminger, M., Leppä, J., Loukonen, V., Makhmutov, V., Mathot, S., McGrath, M.J., Nieminen, T., Olenius, T., Onnela, A., Petäjä, T., Riccobono, F., Riipinen, I., Rissanen, M., Rondo, L., Ruuskanen, T., Santos, F.D., Samela, N., Schallhart, S., Schnitzhofer, R., Seinfeld, J.H., Simon, M., Sipilä, M., Stozhkov, Y., Stratmann, F., Tomé, A., Tröstl, J., Tsagkogeorgas, G., Vaattovaara, P., Viisanen, Y., Virtanen, A., Vrtala, A., Wagner, P.E., Weingartner, E., Wex, H., Williamson, C., Wimmer, D., Ye, P., Yli-Juuti, T., Carslaw, K.S., Kulmala, M., Curtius, J., Baltensperger, U., Worsnop, D.R., Vehkamäki, H., Kirkby, J.: Molecular understanding of sulphuric acid–amine particle nucleation in the atmosphere. *Nature*. **502**, 359–363 (2013)
  17. Myllys, N., Olenius, T., Kurtén, T., Vehkamäki, H., Riipinen, I., Elm, J.: Effect of bisulfate, ammonia, and ammonium on the clustering of organic acids and sulfuric acid. *J. Phys. Chem. A*. **121**, 4812–4824 (2017)
  18. Bianchi, F., Praplan, A.P., Samela, N., Dommen, J., Kürten, A., Ortega, I.K., Schobesberger, S., Junninen, H., Simon, M., Tröstl, J., Jokinen, T., Sipilä, M., Adamov, A., Amorim, A., Almeida, J., Breitenlechner, M., Duplissy, J., Ehrhart, S., Flagan, R.C., Franchin, A., Hakala, J., Hansel, A., Heinritzi, M., Kangasluoma, J., Keskinen, H., Kim, J., Kirkby, J., Laaksonen, A., Lawler, M.J., Lehtipalo, K., Leiminger, M., Makhmutov, V., Mathot, S., Onnela, A., Petäjä, T., Riccobono, F., Rissanen, M.P., Rondo, L., Tomé, A., Virtanen, A., Viisanen, Y., Williamson, C., Wimmer, D., Winkler, P.M., Ye, P., Curtius, J., Kulmala, M., Worsnop, D.R., Donahue, N.M., Baltensperger, U.: Insight into acid–base nucleation experiments by comparison of the chemical composition of positive, negative, and neutral clusters. *Environ. Sci. Technol.* **48**, 13675–13684 (2014)
  19. Schobesberger, S., Franchin, A., Bianchi, F., Rondo, L., Duplissy, J., Kürten, A., Ortega, I.K., Metzger, A., Schnitzhofer, R., Almeida, J., Amorim, A., Dommen, J., Dunne, E.M., Ehn, M., Gagné, S., Ickes, L., Junninen, H., Hansel, A., Kerminen, V.M., Kirkby, J., Kupce, A., Laaksonen, A., Lehtipalo, K., Mathot, S., Onnela, A., Petaja, T., Riccobono, F., Santos, F.D., Sipilä, M., Tomé, A., Tsagkogeorgas, G., Viisanen, Y., Wagner, P.E., Wimmer, D., Curtius, J., Donahue, N.M., Baltensperger, U., Kulmala, M., Worsnop, D.R.: On the composition of ammonia–sulfuric-acid ion clusters during aerosol particle formation. *Atmos. Chem. Phys.* **15**, 55–78 (2015)
  20. Ouyang, H., He, S., Larriba-Andaluz, C., Hogan, C.J.: IMS–MS and IMS–IMS investigation of the structure and stability of dimethylamine-sulfuric acid nanoclusters. *J. Phys. Chem. A*. **119**, 2026–2036 (2015)
  21. Bianchi, F., Tröstl, J., Junninen, H., Frege, C., Henne, S., Hoyle, C.R., Molteni, U., Herrmann, E., Adamov, A., Bukowiecki, N., Chen, X., Duplissy, J., Gysel, M., Hutterli, M., Kangasluoma, J., Kontkanen, J., Kürten, A., Manninen, H.E., Münch, S., Peräkylä, O., Petäjä, T., Rondo, L., Williamson, C., Weingartner, E., Curtius, J., Worsnop, D.R., Kulmala, M., Dommen, J., Baltensperger, U.: New particle formation in the free troposphere: a question of chemistry and timing. *Science*. **352**, 1109–1112 (2016)
  22. Zhang, R., Suh, I., Zhao, J., Zhang, D., Fortner, E., Tie, X., Molina, L., Molina, M.: Atmospheric new particle formation enhanced by organic acids. *Science*. **304**, 1487–1490 (2004)
  23. Elm, J., Passananti, M., Kurtén, T., Vehkamäki, H.: Diamines can initiate new particle formation in the atmosphere. *J. Phys. Chem. A*. **121**, 6155–6164 (2017)
  24. Chen, H., Ezell, M.J., Arquero, K.D., Varner, M.E., Dawson, M.L., Gerber, R.B., Finlayson-Pitts, B.J.: New particle formation and growth from methanesulfonic acid, trimethylamine and water. *Phys. Chem. Chem. Phys.* **17**, 13699–13709 (2015)
  25. Bzdek, B.R., Horan, A.J., Pennington, M.R., DePalma, J.W., Zhao, J., Jen, C.N., Hanson, D.R., Smith, J.N., McMurry, P.H., Johnston, M.V.: Quantitative and time-resolved nanoparticle composition measurements during new particle formation. *Faraday Discuss.* **165**, 25–43 (2013)
  26. Bzdek, B.R., DePalma, J.W., Johnston, M.V.: Mechanisms of atmospherically relevant cluster growth. *Acc. Chem. Res.* **50**, 1965–1975 (2017)
  27. Weber, R.J., Marti, J.J., McMurry, P.H., Eisele, F.L., Tanner, D.J., Jefferson, A.: Measured atmospheric new particle formation rates: implications for nucleation mechanisms. *Chem. Eng. Commun.* **151**, 53–64 (1996)
  28. Kulmala, M., Pirjola, L., Mäkelä, J.M.: Stable sulphate clusters as a source of new atmospheric particles. *Nature*. **404**, 66–69 (2000)

29. Ortega, I.K., Kurtén, T., Vehkamäki, H., Kulmala, M.: The role of ammonia in sulfuric acid ion induced nucleation. *Atmos. Chem. Phys.* **8**, 2859–2867 (2008)
30. Loukonen, V., Kurtén, T., Ortega, I.K., Vehkamäki, H., Pádua, A.A.H., Sellegri, K., Kulmala, M.: Enhancing effect of dimethylamine in sulfuric acid nucleation in the presence of water – a computational study. *Atmos. Chem. Phys.* **10**, 4961–4974 (2010)
31. Tsona, N.T., Henschel, H., Bork, N., Loukonen, V., Vehkamäki, H.: Structures, hydration, and electrical mobilities of bisulfate ion–sulfuric acid–ammonia/dimethylamine clusters: a computational study. *J. Phys. Chem. A* **119**, 9670–9679 (2015)
32. Henschel, H., Kurtén, T., Vehkamäki, H.: Computational study on the effect of hydration on new particle formation in the sulfuric acid/ammonia and sulfuric acid/dimethylamine systems. *J. Phys. Chem. A* **120**, 1886–1896 (2016)
33. Ahlm, L., Yli-Juuti, T., Schobesberger, S., Praplan, A.P., Kim, J., Tikkanen, O.P., Lawler, M.J., Smith, J.N., Tröstl, J., Acosta Navarro, J.C., Baltensperger, U., Bianchi, F., Donahue, N.M., Duplissy, J., Franchin, A., Jokinen, T., Keskinen, H., Kirkby, J., Kürten, A., Laaksonen, A., Lehtipalo, K., Petäjä, T., Riccobono, F., Rissanen, M.P., Rondo, L., Schallhart, S., Simon, M., Winkler, P.M., Worsnop, D.R., Virtanen, A., Riipinen, I.: Modeling the thermodynamics and kinetics of sulfuric acid-dimethylamine-water nanoparticle growth in the CLOUD chamber. *Aerosol Sci. Technol.* **50**, 1017–1032 (2016)
34. Elm, J.: Elucidating the limiting steps in sulfuric acid–base new particle formation. *J. Phys. Chem. A* **121**, 8288–8295 (2017)
35. Olenius, T., Halonen, R., Kurtén, T., Henschel, H., Kupiainen-Määttä, O., Ortega, I.K., Jen, C.N., Vehkamäki, H., Riipinen, I.: New particle formation from sulfuric acid and amines: comparison of mono-, di-, and trimethylamines. *J. Geophys. Res. Atmos.* **122**, 7103–7118 (2017)
36. DePalma, J.W., Bzdek, B.R., Doren, D.J., Johnston, M.V.: Structure and energetics of nanometer size clusters of sulfuric acid with ammonia and dimethylamine. *J. Phys. Chem. A* **116**, 1030–1040 (2012)
37. Kildgaard, J.V., Mikkelsen, K.V., Bilde, M., Elm, J.: Hydration of atmospheric molecular clusters: a new method for systematic configurational sampling. *J. Phys. Chem. A* **122**, 5026–5036 (2018)
38. Bzdek, B.R., Ridge, D.P., Johnston, M.V.: Size-dependent reactions of ammonium bisulfate clusters with dimethylamine. *J. Phys. Chem. A* **114**, 11638–11644 (2010)
39. Bzdek, B.R., Ridge, D.P., Johnston, M.V.: Amine exchange into ammonium bisulfate and ammonium nitrate nuclei. *Atmos. Chem. Phys.* **10**, 3495–3503 (2010)
40. Bzdek, B.R., DePalma, J.W., Ridge, D.P.: Fragmentation energetics of clusters relevant to atmospheric new particle formation. *J. Am. Chem. Soc.* **135**, 3276–3285 (2013)
41. Lv, S.-S., Miao, S.-K., Ma, Y., Zhang, M.-M., Wen, Y., Wang, C.-Y., Zhu, Y.-P., Huang, W.: Properties and atmospheric implication of methylamine–sulfuric acid–water clusters. *J. Phys. Chem. A* **119**, 8657–8666 (2015)
42. Henschel, H., Navarro, J.C.A., Yli-Juuti, T., Kupiainen-Määttä, O., Olenius, T., Ortega, I.K., Clegg, S.L., Kurtén, T., Riipinen, I., Vehkamäki, H.: Hydration of atmospherically relevant molecular clusters: computational chemistry and classical thermodynamics. *J. Phys. Chem. A* **118**, 2599–2611 (2014)
43. Miller, Y., Chaban, G.M., Zhou, J., Asmis, K.R., Neumark, D.M., Gerber, R.B.: Vibrational spectroscopy of  $(\text{SO}_4^{2-}) \cdot (\text{H}_2\text{O})_n$  clusters,  $n=1-5$ : harmonic and anharmonic calculations and experiment. *J. Chem. Phys.* **127**, 094305 (2007)
44. Yacovitch, T.I., Heine, N., Brieger, C., Wende, T.: Communication: vibrational spectroscopy of atmospherically relevant acid cluster anions: bisulfate versus nitrate core structures. *J. Chem. Phys.* **136**, 241102 (2012)
45. Yacovitch, T.I., Heine, N., Brieger, C., Wende, T., Hock, C., Neumark, D.M., Asmis, K.R.: Vibrational spectroscopy of bisulfate/sulfuric acid/water clusters: structure, stability, and infrared multiple-photon dissociation intensities. *J. Phys. Chem. A* **117**, 7081–7090 (2013)
46. Hou, G.L., Lin, W., Deng, S.H.M., Zhang, J., Zheng, W.J., Paesani, F., Wang, X.B.: Negative ion photoelectron spectroscopy reveals thermodynamic advantage of organic acids in facilitating formation of bisulfate ion clusters: atmospheric implications. *J. Phys. Chem. Lett.* **4**, 779–785 (2013)
47. Heine, N., Asmis, K.R.: Cryogenic ion trap vibrational spectroscopy of hydrogen-bonded clusters relevant to atmospheric chemistry. *Int. Rev. Phys. Chem.* **34**, 1–34 (2014)
48. Johnson, C.J., Johnson, M.A.: Vibrational spectra and fragmentation pathways of size-selected,  $\text{D}_2$ -tagged ammonium/methylammonium bisulfate clusters. *J. Phys. Chem. A* **117**, 13265–13274 (2013)
49. Wiley, W.C., McLaren, I.H.: Time-of-flight mass spectrometer with improved resolution. *Rev. Sci. Instrum.* **26**, 1150–1157 (1955)
50. Frisch, M.J., Trucks, G.W., Schlegel, H.B., Scuseria, G.E., Robb, M.A., Cheeseman, J.R., Scalmani, G., Barone, V., Mennucci, B., Petersson, G.A., Nakatsuji, H., Caricato, M., Li, Xiaosong, Hratchian, H.P., Izmaylov, A.F., Bloino, J., Zheng, G., Sonnenberg, J.L., Hada, M., Ehara, M., Toyota, K., Fukuda, R., Hasegawa, J., Ishida, M., Nakajima, T., Honda, Y., Kitao, O., Nakai, H., Vreven, T., Montgomery Jr., J.A., Peralta, J.E., Ogliaro, F., Bearpark, M.J., Heyd, J., Brothers, E.N., Kudin, K.N., Staroverov, V.N., Kobayashi, R., Normand, J., Raghavachari, K., Rendell, A.P., Burant, J.C.: Gaussian 09. Gaussian, Inc., Wallingford (2009)
51. Waller, S.E., Yang, Y., Castracane, E., Racow, E.E., Kreinbihl, J.J., Nickson, K.A., Johnson, C.J.: The interplay between hydrogen bonding and coulombic forces in determining the structure of sulfuric acid-amine clusters. *J. Phys. Chem. Lett.* **9**, 1216–1222 (2018)
52. Yang, Y., Waller, S.E., Kreinbihl, J.J., Johnson, C.J.: Direct link between structure and hydration in ammonium and aminium bisulfate clusters implicated in atmospheric new particle formation. *J. Phys. Chem. Lett.* **9**, 5647–5652 (2018)
53. Johnson, C.J., Fournier, J.A., Wolke, C.T., Johnson, M.A.: Ionic liquids from the bottom up: local assembly motifs in  $[\text{EMIM}][\text{BF}_4]$  through cryogenic ion spectroscopy. *J. Chem. Phys.* **139**, 224305 (2013)
54. Froyd, K.D., Lovejoy, E.R.: Bond energies and structures of ammonia–sulfuric acid positive cluster ions. *J. Phys. Chem. A* **116**, 5886–5899 (2012)
55. DePalma, J.W., Bzdek, B.R., Ridge, D.P., Johnston, M.V.: Activation barriers in the growth of molecular clusters derived from sulfuric acid and ammonia. *J. Phys. Chem. A* **118**, 11547–11554 (2014)
56. Bzdek, B.R., DePalma, J.W., Ridge, D.P., Laskin, J., Johnston, M.V.: Fragmentation energetics of clusters relevant to atmospheric new particle formation. *J. Am. Chem. Soc.* **135**, 3276–3285 (2013)
57. Hogan, C.J., De la Mora, J.F.: Ion-pair evaporation from ionic liquid clusters. *J. Am. Soc. Mass Spectrom.* **21**, 1382–1386 (2010)
58. Fernández-García, J., de la Mora, J.F.: Measuring the effect of ion-induced drift-gas polarization on the electrical mobilities of multiply-charged ionic liquid nanodrops in air. *J. Am. Soc. Mass Spectrom.* **24**, 1872–1889 (2013)
59. Thomas, J.M., He, S., Larriba-Andaluz, C., DePalma, J.W., Johnston, M.V., Hogan Jr., C.J.: Ion mobility spectrometry-mass spectrometry examination of the structures, stabilities, and extents of hydration of dimethylamine-sulfuric acid clusters. *Phys. Chem. Chem. Phys.* **18**, 22962–22972 (2016)
60. Passananti, M., Zapadinsky, E., Zanca, T., Kangasluoma, J., Myllys, N., Rissanen, M.P., Kurtén, T., Ehn, M., Attoui, M., Vehkamäki, H.: How well can we predict cluster fragmentation inside a mass spectrometer? *Chem. Commun.* **55**, 5946–5949 (2019)
61. Bzdek, B.R., Ridge, D.P., Johnston, M.V.: Amine reactivity with charged sulfuric acid clusters. *Atmos. Chem. Phys.* **11**, 8735–8743 (2011)
62. Lehtipalo, K., Rondo, L., Kontkanen, J., Schobesberger, S., Jokinen, T., Sarnela, N., Kürten, A., Ehrhart, S., Franchin, A., Nieminen, T., Riccobono, F., Sipilä, M., Yli-Juuti, T., Duplissy, J., Adamov, A., Ahlm, L., Almeida, J., Amorim, A., Bianchi, F., Breitenlechner, M., Dommen, J., Downard, A.J., Dunne, E.M., Flagan, R.C., Guida, R., Hakala, J., Hansel, A., Jud, W., Kangasluoma, J., Kerminen, V.-M., Keskinen, H., Kim, J., Kirkby, J., Kupc, A., Kupiainen-Määttä, O., Laaksonen, A., Lawler, M.J., Leiminger, M., Mathot, S., Olenius, T., Ortega, I.K., Onnela, A., Petäjä, T., Praplan, A., Rissanen, M.P., Ruuskanen, T., Santos, F.D., Schallhart, S., Schnitzhofer, R., Simon, M., Smith, J.N., Tröstl, J., Tsagkogeorgas, G., Tomé, A., Vaattovaara, P., Vehkamäki, H., Virtala, A.E., Wagner, P.E., Williamson, C., Wimmer, D., Winkler, P.M., Virtanen, A., Donahue, N.M., Carslaw, K.S., Baltensperger, U., Riipinen, I., Curtius, J., Worsnop, D.R., Kulmala, M.: The effect of acid–base clustering and ions on the growth of atmospheric nano-particles. *Nat. Commun.* **7**, 11594 (2016)
63. Kupiainen, O., Ortega, I.K., Kurtén, T., Vehkamäki, H.: Amine substitution into sulfuric acid - ammonia clusters. *Atmos. Chem. Phys.* **12**, 3591–3599 (2012)
64. Morrell, T.E., Shields, G.C.: Atmospheric implications for formation of clusters of ammonium and 1–10 water molecules. *J. Phys. Chem. A* **114**, 4266–4271 (2010)